SUPPLEMENTARY MATERIAL

Phytoplankton Tune Local pH to Actively Modulate Circadian Gravitactic Behavior

Arkajyoti Ghoshal[1], Soumitree Mishra[1], Jayabrata Dhar[2], Hans-Peter Grossart[3,4], and Anupam Sengupta[1,5]*

[1]Physics of Living Matter, Department of Physics and Materials Science, University of Luxembourg, 162A, Avenue de la Faïencerie, L-1511 Luxembourg City, Luxembourg

[2]Department of Mechanical Engineering, National Institute of Technology Durgapur, 713203, India

[3]Department of Plankton and Microbial Ecology, Leibniz Institute of Freshwater Ecology and Inland Fisheries, Zur alten Fischerhuette 2, 16775 Stechlin, Gemany

[4]Institute of Biochemistry and Biology, Potsdam University, Maulbeerallee 2, D-14469 Potsdam, Germany

[5]Institute for Advanced Studies, University of Luxembourg, 2 Avenue de l'Université, L-4365, Esch-sur-Alzette, Luxembourg

* To whom correspondence should be addressed: anupam.sengupta@uni.lu

This file contains:

Supplementary figures and captions for Figures S1 to S19

Supplementary Figures

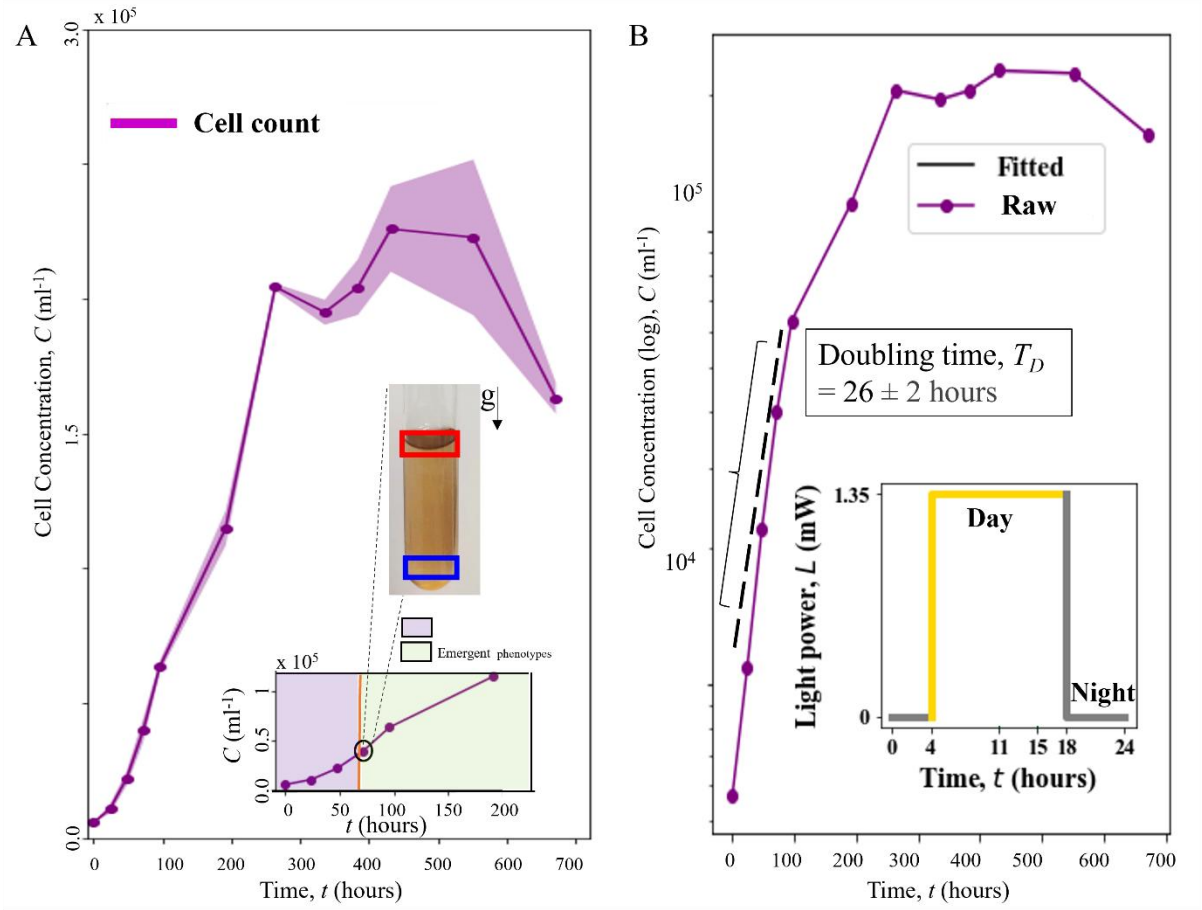

Fig. S1. Quantification of doubling time from HA 452 growth curve. In order to compute the doubling time, the growth curve shown in Fig.1 A (main text), was plotted in a logarithmic scale, shown in purple. The exponential phase of growth is fitted to an exponential function (shown in black lines). The coefficient of the exponent gives us the growth rate from which doubling time is calculated (Materials and Methods). Doubling time, T_D ranges from 24 to 28 hours which matches well with ranges of other phytoplankton mentioned in literature (see main text). **(A)** Growth curve of *Heterosigma akashiwo* (HA) 452 culture (number of replicates, n = 4), grown under a 14 h (light) – 10 h (dark) cycle (inset, top-left) at 22°C within a vertical culture column is ~70mm. The inset (bottom-right) marks the timepoint at which the vertically segregated sub-populations emerge, visualized by the uniform hue of the homogeneous cell culture (upper inset panel of culture at 96 h after inoculation), compared to the vertical gradient of hue observed for the negatively gravitactic cell population (before 96 h). The darker hue on the upper part of the culture and lighter below indicate the presence of higher number of cells near the top.

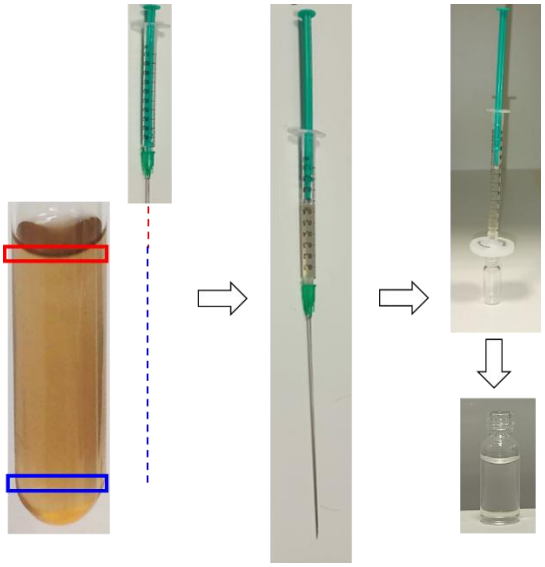

Fig. S2. Generation of filtrate from a cell culture. To generate filtrates, cell samples are collected from a growing culture (left most panel) from either the top (red box) or bottom (blue box) region. Collection is done using a needle and syringe (Materials and Methods). The red or blue dotted lines indicate the depth of needle for collection of top or bottom sample. Once samples are collected (middle panel), they are passed through a 1 μm pore sized syringe filter (right panel, top) and collected into a glass vial (right panel, bottom). These are then used for measuring pH, nutrients, and response of cells in presence or absence of same or opposite filtrates.

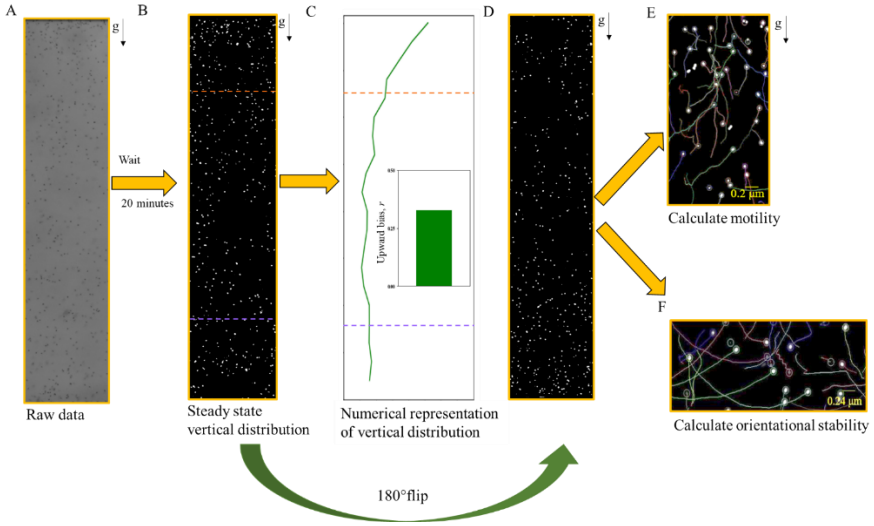

Fig. S3. Image analysis pipeline. This figure shows a general pipeline used for analyzing raw data (panel **(A)**) and extract parameters like upward bias, motility and stability. These parameters have been mentioned and used multiple times throughout the paper and uses the same approach as shown here. First one takes the raw data and then binarizes it for downstream analyses. **(B)** shows one such binarized image of cells in a millifluidic chamber, after 20 minutes from the point of insertion. **(C)** shows how the binarized input is used to compute vertical distribution, shown in green line (for details, see Materials and methods). From this, upward bias value is calculated by considering the cell concentration in the top and bottom $1/5^{th}$ of the chamber, indicated by the dark orange and lavender dotted lines. **(D)** To calculate motility and orientational stability, after an equilibriation time (here 20 minutes), the chamber is flipped by 180 degrees. Cells at the top pre-flip are now at the bottom and start to swim up. **(E)** As cells swim up, a short video is captured which is analysed to obtain swimming trajectories from which motility parameter like speed and swimming direction can be obtained for individual cells. **(F)** Flipping the chamber also changes cellular orientation from their stable configuration and they start to reorient, as shown by the arc-like trajectories.

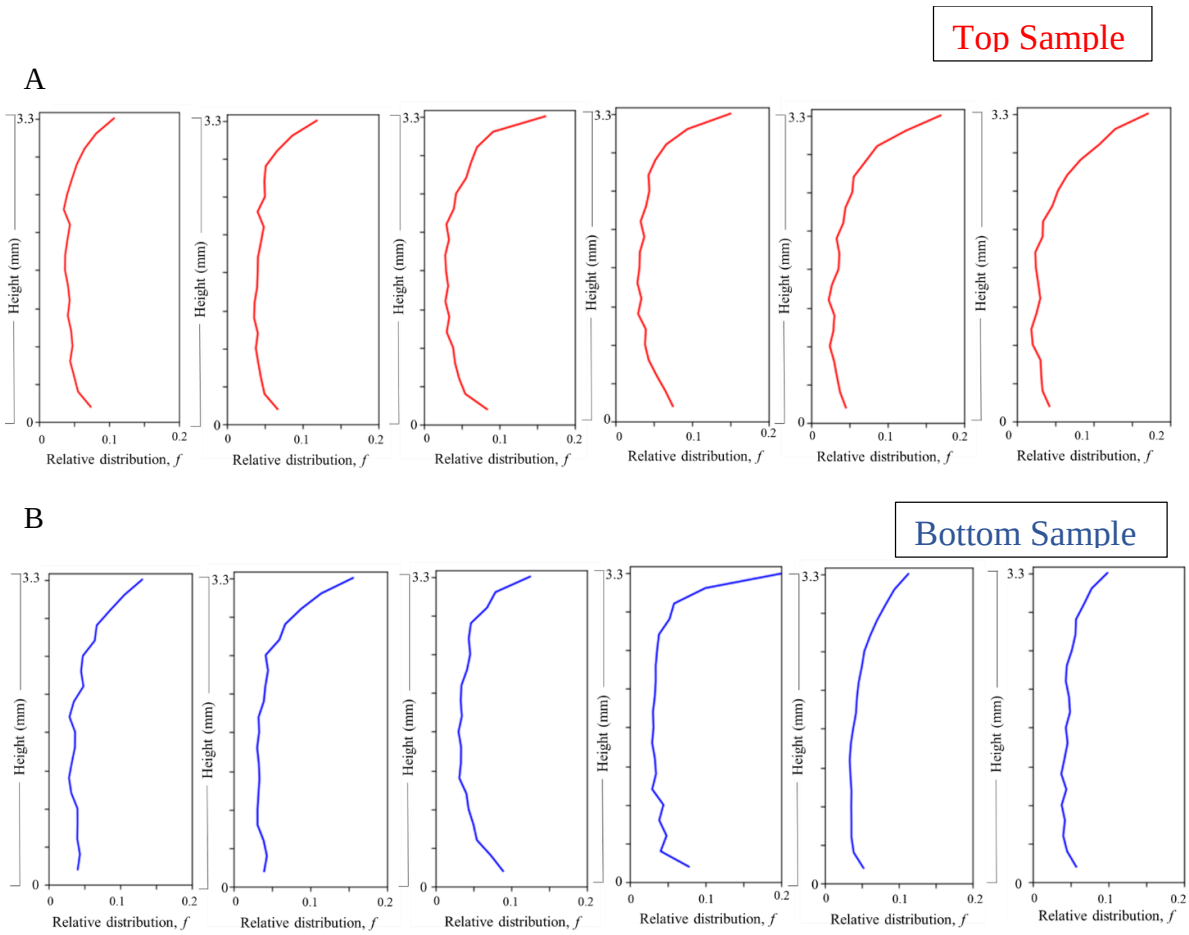

Fig. S4. Vertical distribution of cells in a multifluidic chamber. To observe the vertical distribution of cells, samples were collected from top (red) and bottom (blue) and placed into a multifluidic chamber of vertical height 3.3 mm. After 20 minutes, the entire height was imaged for subsequent cell count. **(A)** shows the distribution of top cells with each panel corresponding to one replicate (of 6 replicates, 3 biological replicates each having 2 technical replicates). **(B)** shows the same but for bottom cells. First two panels show technical replicates of the first biological replicate and the rest follows that order.

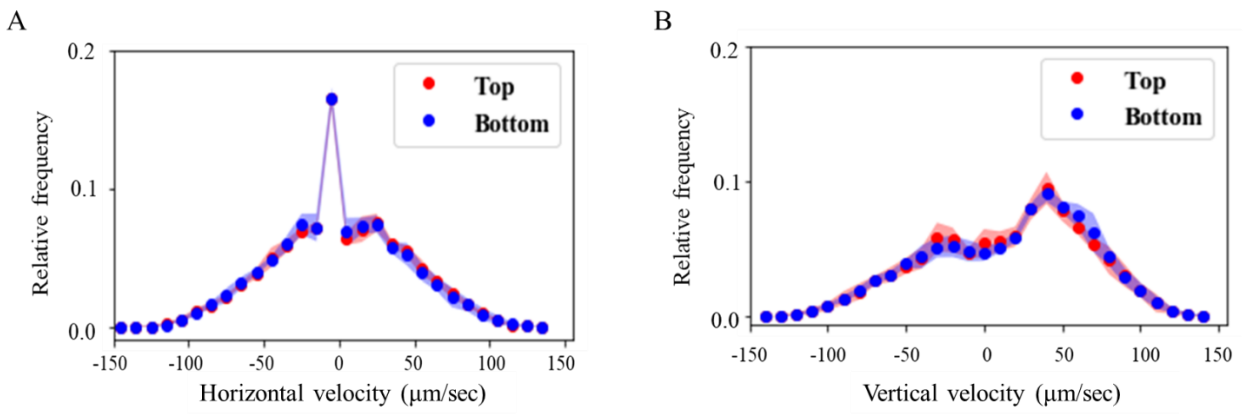

Fig. S5. Motility parameters of cells. While Fig. 1 H of main text shows that the mean absolute swimming speed of top and bottom cells are similar, we also wanted to see if their directionality remains similar identical as well (reason in main text). **(A)** shows the relative distribution of mean horizontal swimming speed of all 6 replicates for top and bottom cells (red and blue respectively). Horizontal velocity is divided into two sections about 0. Cells swimming towards their right from their initial position is assigned positive velocity and those swimming left are assigned negative velocities. Results indicate that the majority population of both samples have a mean horizontal speed of 0 μm/s, meaning that on a population scale, cells do not show much displacement in the horizontal direction. **(B)** shows the relative distribution of mean vertical swimming speed of the same. Vertical velocity is divided into two sections about 0. Cells swimming against gravity from their initial position is assigned positive velocity and those swimming towards, are assigned negative velocities. (Direction of gravity, *g*, is shown by the black arrows to the right of both panels) Mean vertical velocity of both samples peak at around 35 μm/s, meaning that the population as a whole move actively against gravity, precisely in the negative vertical direction.

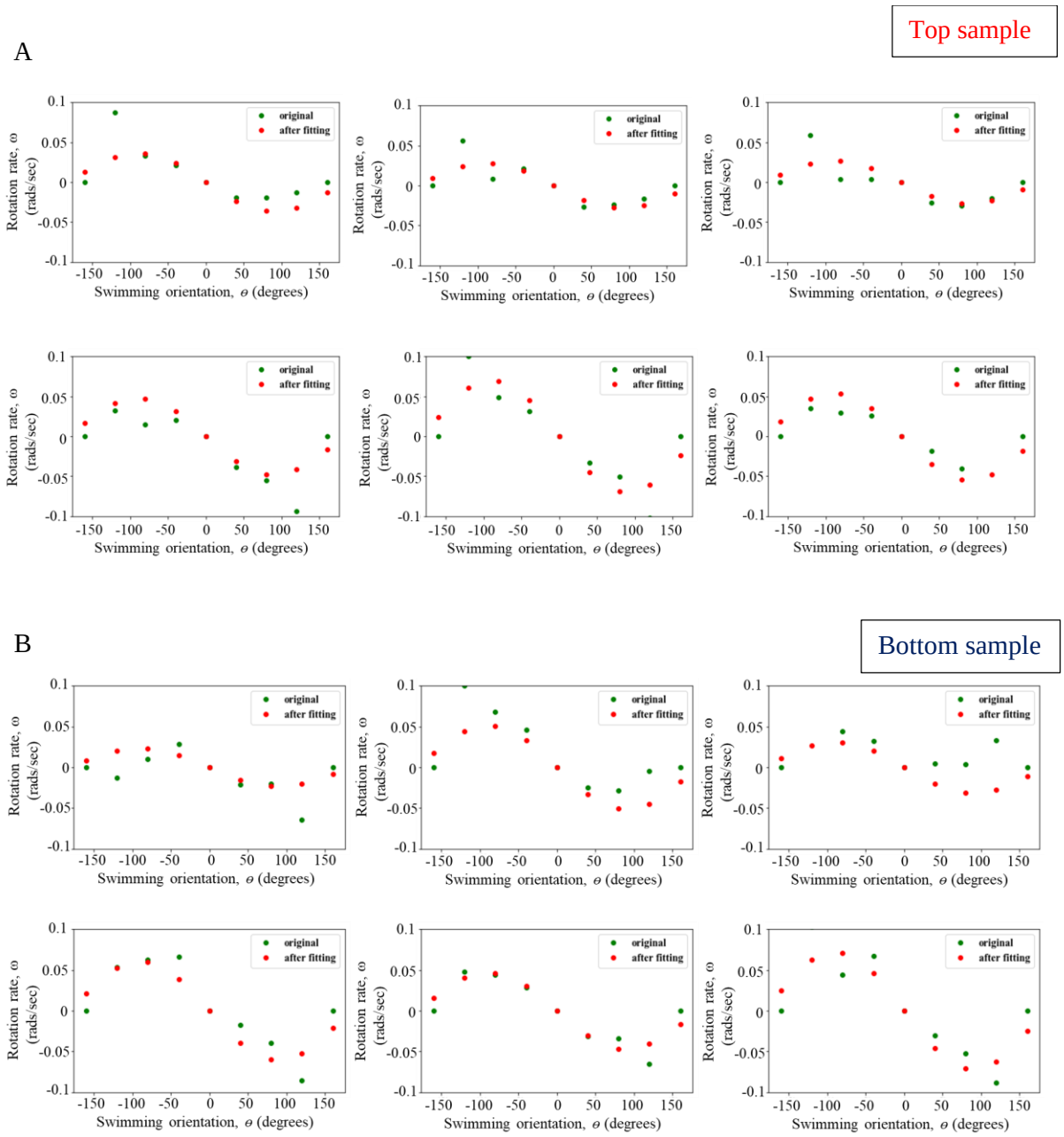

Fig. S6. Quantification of the orientational stability of cell samples. To compute the stability of top and bottom samples, rotation rate (ω) of cells were plotted as a function of the instantaneous angular direction (θ). The time of experiment was day (11 hours). **(A)** shows the stability of top cells with each panel corresponding to one replicate. Red dots correspond to experimental data and green dots to the sinusoidal curve obtained by fitting a sinusoid to the experimental data. **(B)** shows the same but for bottom cells. The amplitude, A of the fitted curve was used to obtain the reorientation timescale, B as $B = \frac{1}{2A}$. Note that there are 12 replicates: 3 biological replicates x 2 technical replicates x 2 subreplicates, where 1 subreplicate is obtained by imaging 1 technical replicate for two consecutive flips, as detailed in the Materials and methods section. Here the subreplicates per technical replicate has been combined together, thus showing a total of 3x2x1= 6 plots.

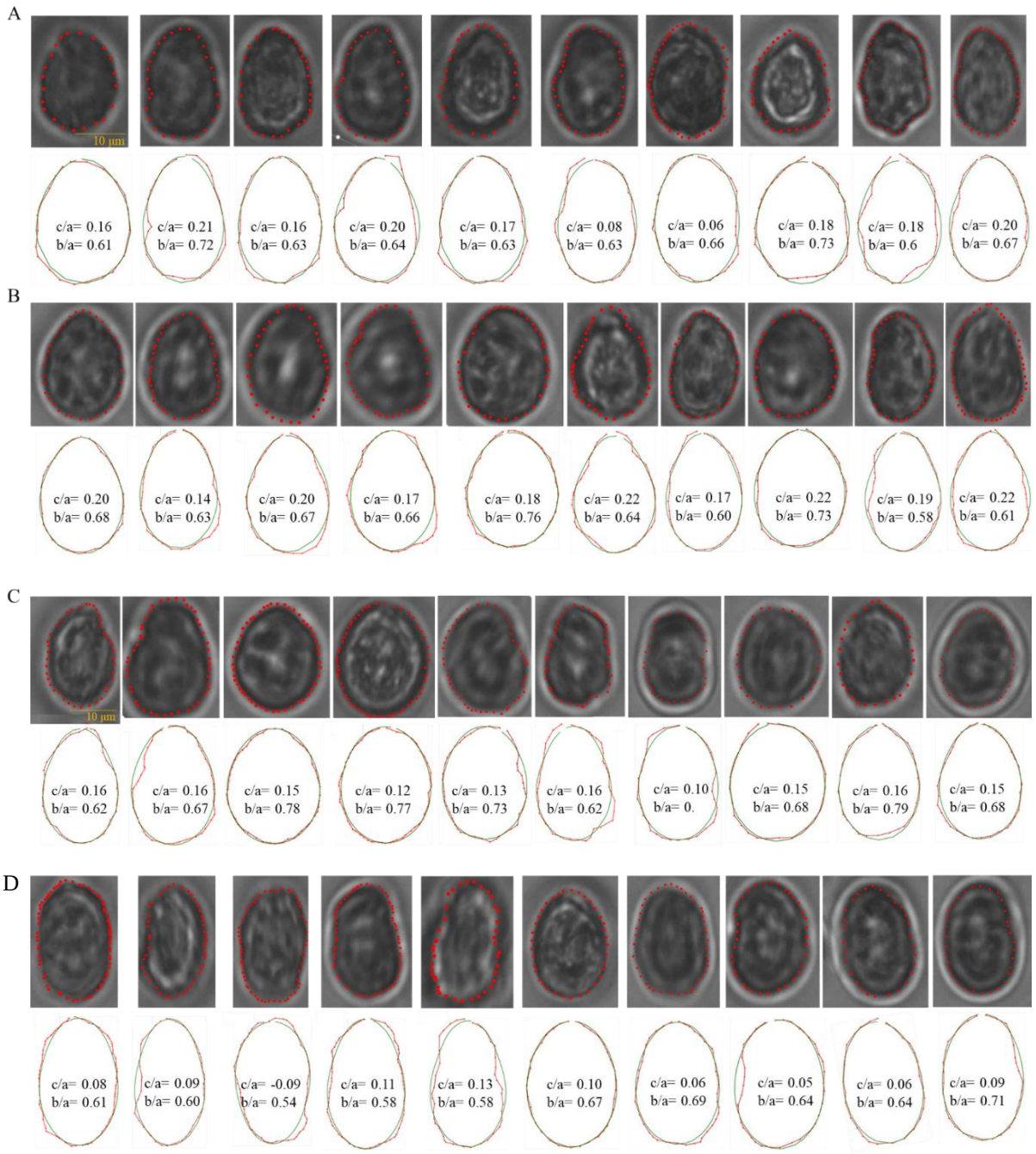

Fig. S7. Quantification of morphological parameters of top cells. The top row of each panel shows phase contrast images of top cells (N = 10). The external contour of each cell was marked, and co-ordinates were extracted. These were then fed into an image analysis pipeline to fit each contour with a fore-aft asymmetric ellipse. The *c/a* parameter is a quantification of this asymmetry. Panels A to D represents distinct time points of 0, 20, 60 and 120 min.

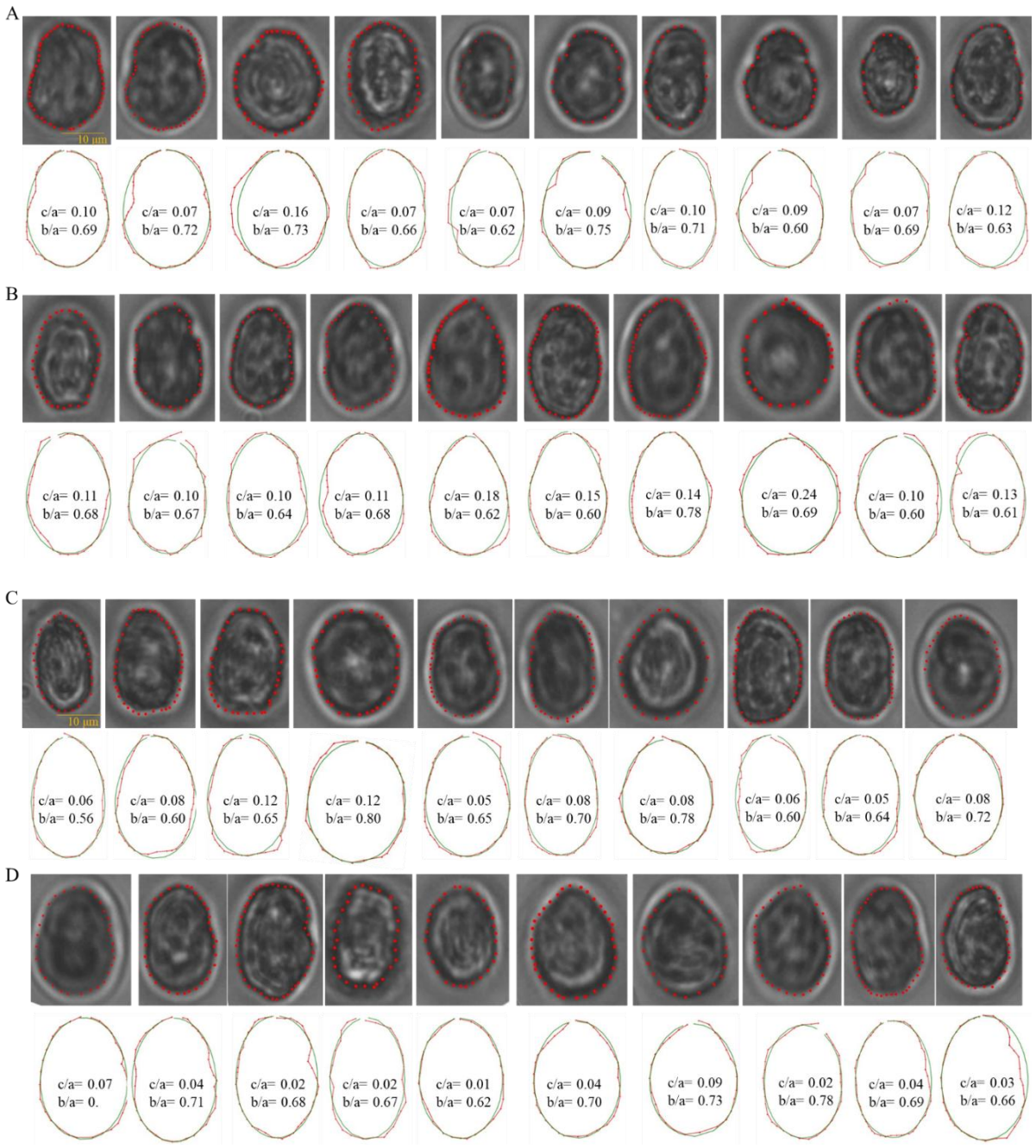

Fig. S8. Quantification of morphological parameters of bottom cells. The top row of each panel shows phase contrast images of bottom cells (N = 10). The external contour of each cell was marked, and co-ordinates were extracted. These were then fed into an image analysis pipeline to fit each contour with a fore-aft asymmetric ellipse. The *c/a* parameter is a quantification of this asymmetry. Panels A to D represents distinct time points of 0, 20, 60 and 120 min.

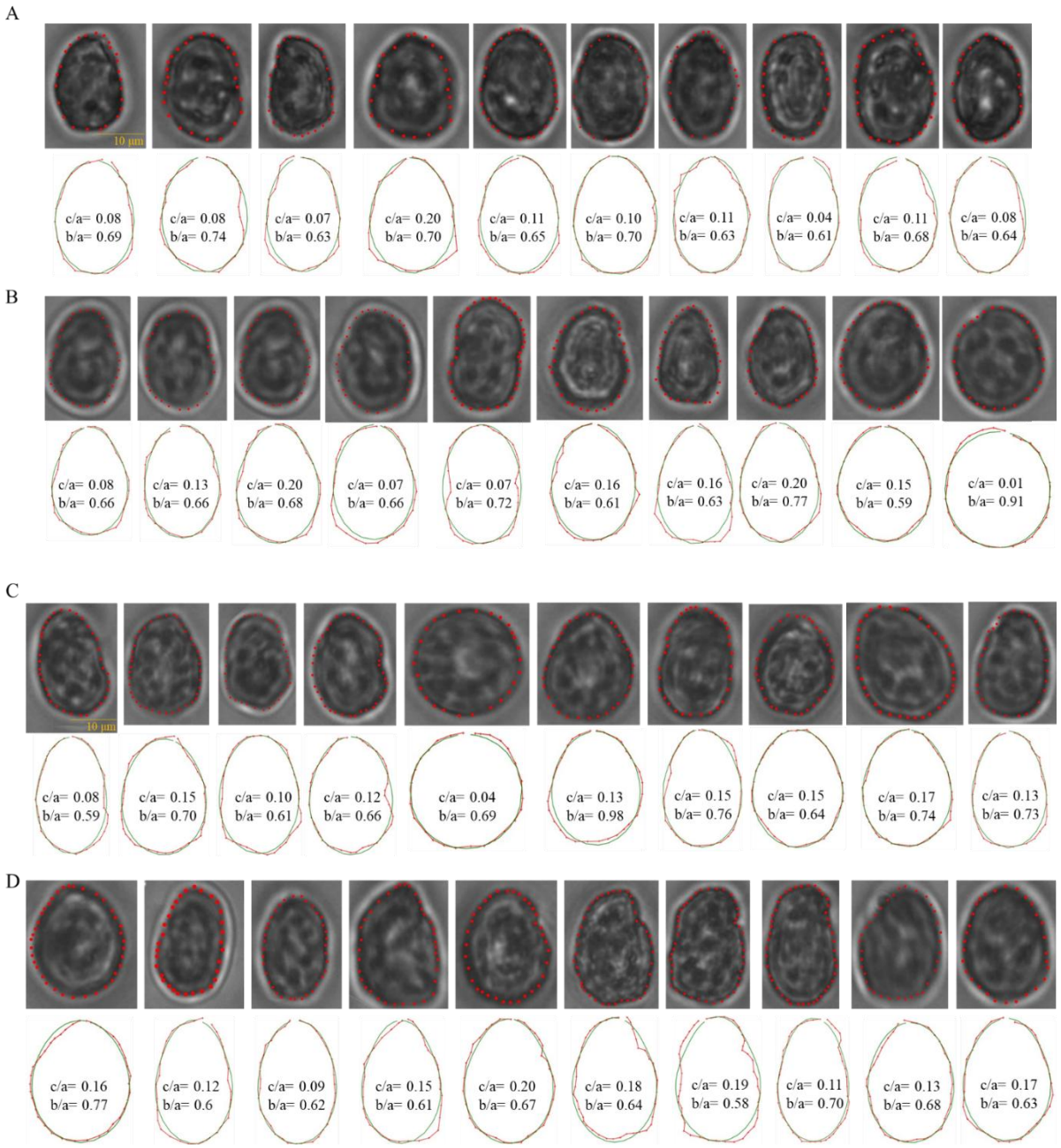

Fig. S9. Quantification of morphological parameters of mixed cells. The top row of each panel shows phase contrast images of 50:50 mixed cells (N = 10). The external contour of each cell was marked, and co-ordinates were extracted. These were then fed into an image analysis pipeline to fit each contour with a fore-aft asymmetric ellipse. The *c/a* parameter is a quantification of this asymmetry. Panels A to D represents distinct time points of 0, 20, 60 and 120 min.

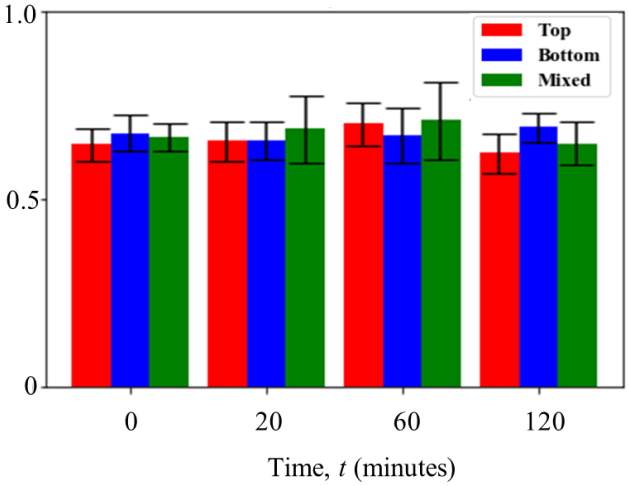

Fig. S10. *b/a* values of cells over time. Complementing the *c/a* values shown in main text, this figure shows the *b/a* values, the ratio of the minor to major semi axis, that gives an idea of the shape of cells. A value of 0 means cells are highly asymmetric, while that of 1 means highly rounded cells. For top cells (red bar), the mean (± s.d.) values over 0, 20, 60 and 120 minutes are 0.65 ± 0.04, 0.66 ± 0.05, 0.7 ± 0.06 and 0.62 ± 0.05. For bottom cells (blue bar), they are 0.68 ± 0.05, 0.66 ± 0.05, 0.67 ± 0.07 and 0.7 ± 0.04. For mixed cells (green bar), they are 0.66 ± 0.04, 0.69 ± 0.09, 0.7 ± 0.1 and 0.65 ± 0.06.

Top cells + Top filtrate (*TT*)

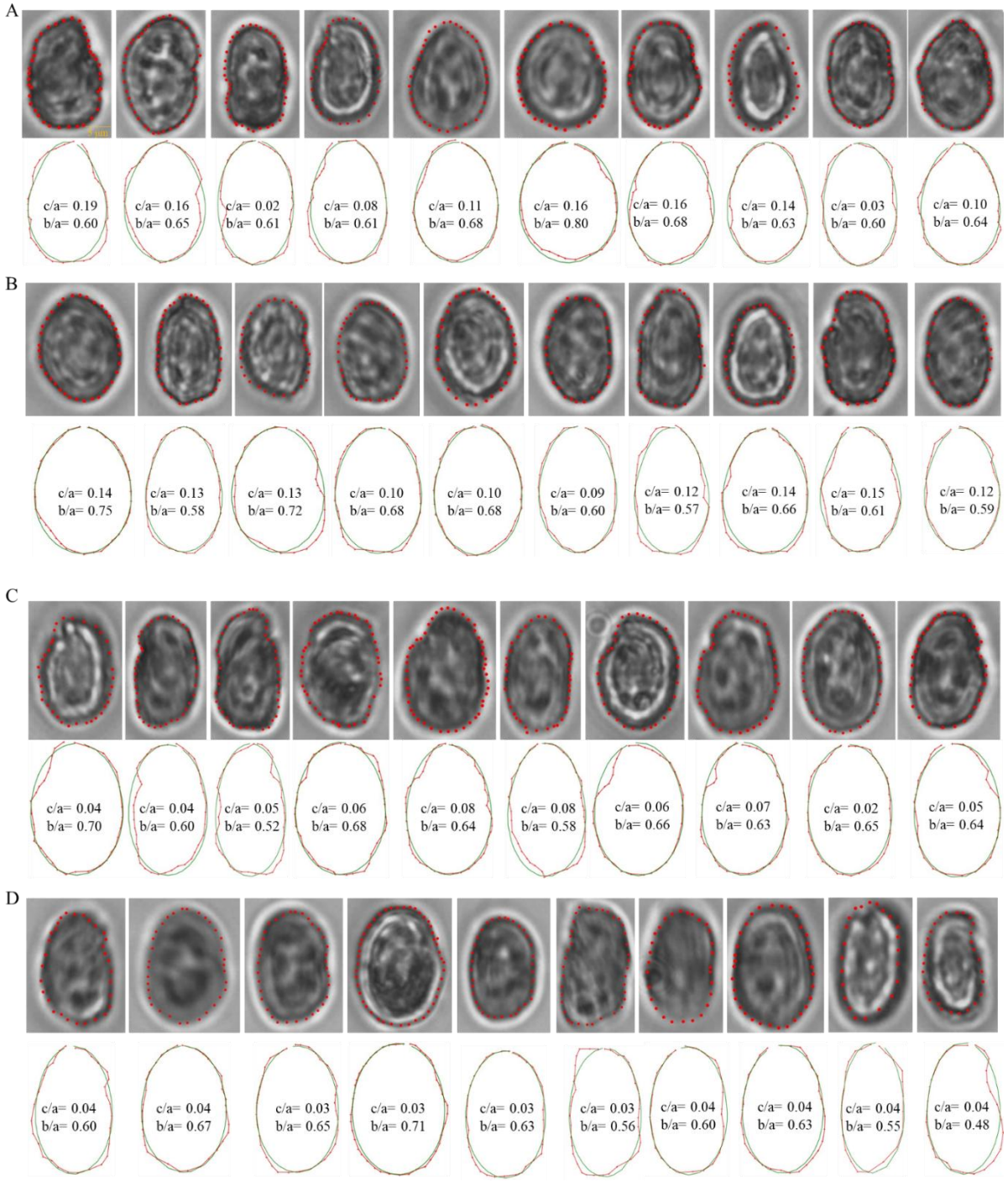

Fig. S11. Quantification of morphological parameters of top cells in top filtrate [*T*, *T*]. The top row of each panel shows phase contrast images of top cells in presence of top filtrate (N = 10). The external contour of each cell was marked, and co-ordinates were extracted. These were then fed into an image analysis pipeline to fit each contour with a fore-aft asymmetric ellipse. The *c/a* parameter is a quantification of this asymmetry. Panels A to D represents distinct time points of 0, 20, 60 and 120 min.

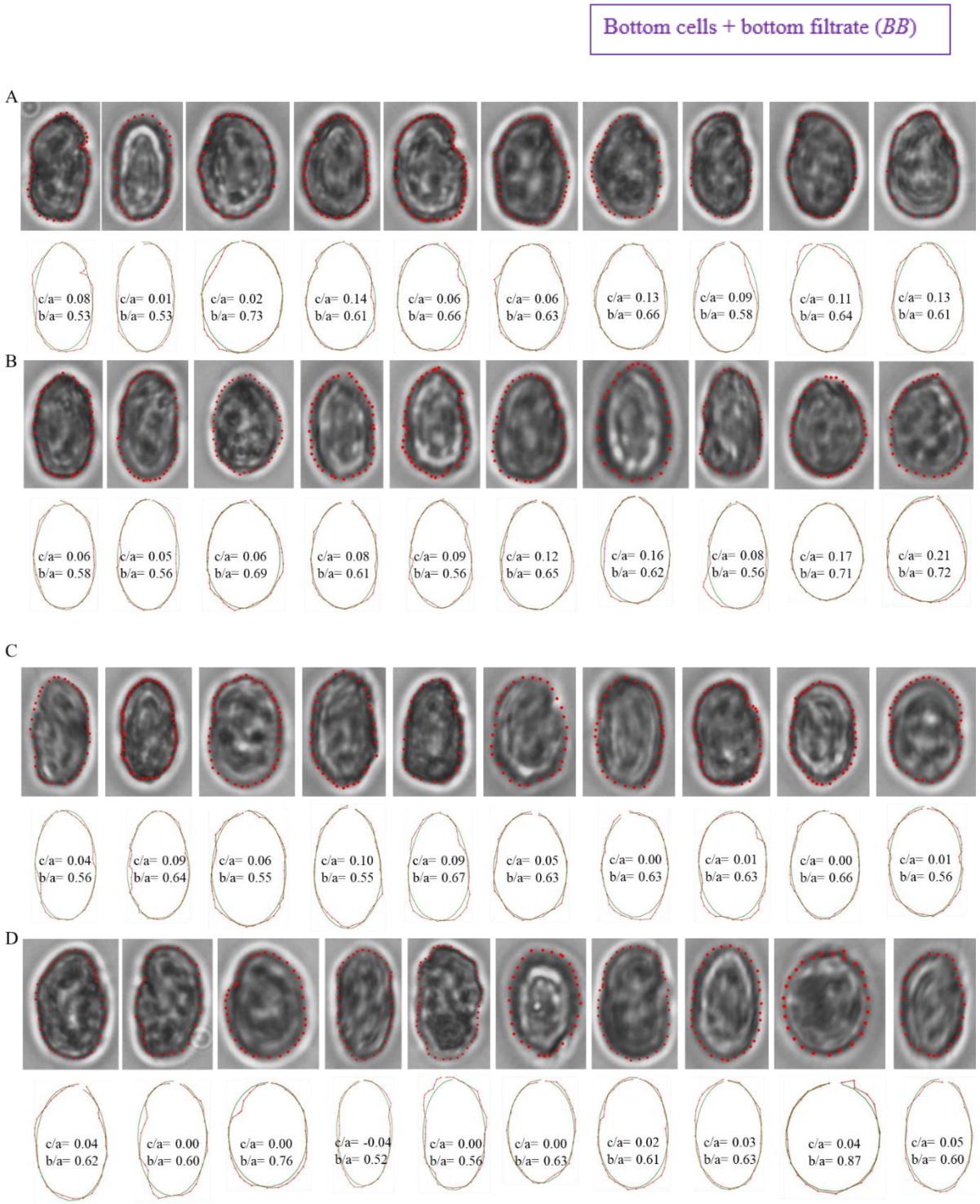

Fig. S12. Quantification of morphological parameters of bottom cells in bottom filtrate *[B, B]*. The top row of each panel shows phase contrast images of top cells in presence of top filtrate (*N* = 10). The external contour of each cell was marked, and co-ordinates were extracted. These were then fed into an image analysis pipeline to fit each contour with a fore-aft asymmetric ellipse. The *c/a* parameter is a quantification of this asymmetry. Panels A to D represents distinct time points of 0, 20, 60 and 120 min.

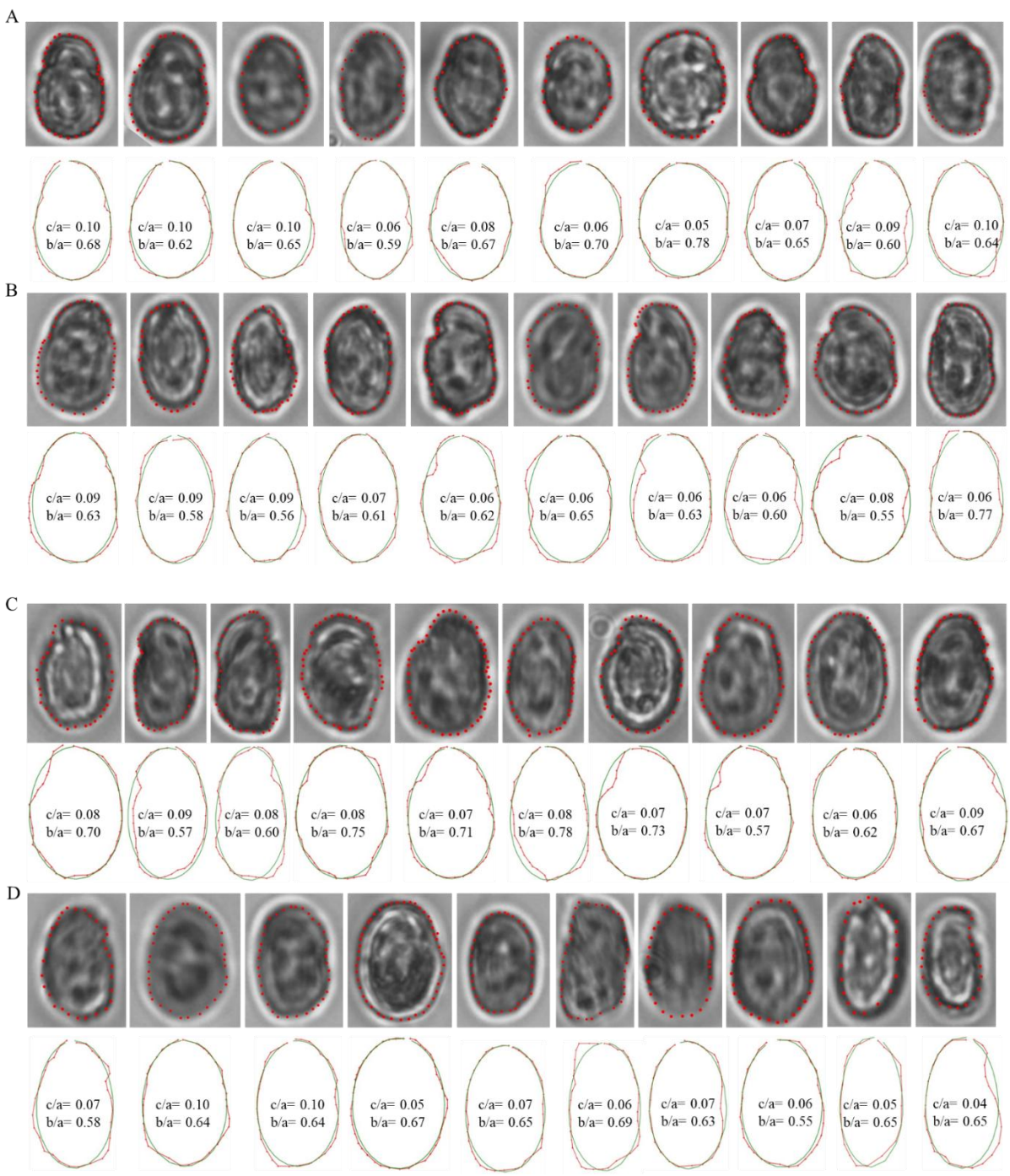

Fig. S13. Quantification of morphological parameters of top cells in bottom filtrate *[B, T]*. The top row of each panel shows phase contrast images of top cells in presence of top filtrate (N = 10). The external contour of each cell was marked, and co-ordinates were extracted. These were then fed into an image analysis pipeline to fit each contour with a fore-aft asymmetric ellipse. The *c/a* parameter is a quantification of this asymmetry. Panels A to D represents distinct time points of 0, 20, 60 and 120 min.

Bottom cells + Top filtrate (*TB*)

Fig. S14. Quantification of morphological parameters of bottom cells in top filtrate *[T, B]*. The top row of each panel shows phase contrast images of top cells in presence of top filtrate ($N = 10$). The external contour of each cell was marked, and co-ordinates were extracted. These were then fed into an image analysis pipeline to fit each contour with a fore-aft asymmetric ellipse. The *c/a* parameter is a quantification of this asymmetry. Panels A to D represents distinct time points of 0, 20, 60 and 120 min.

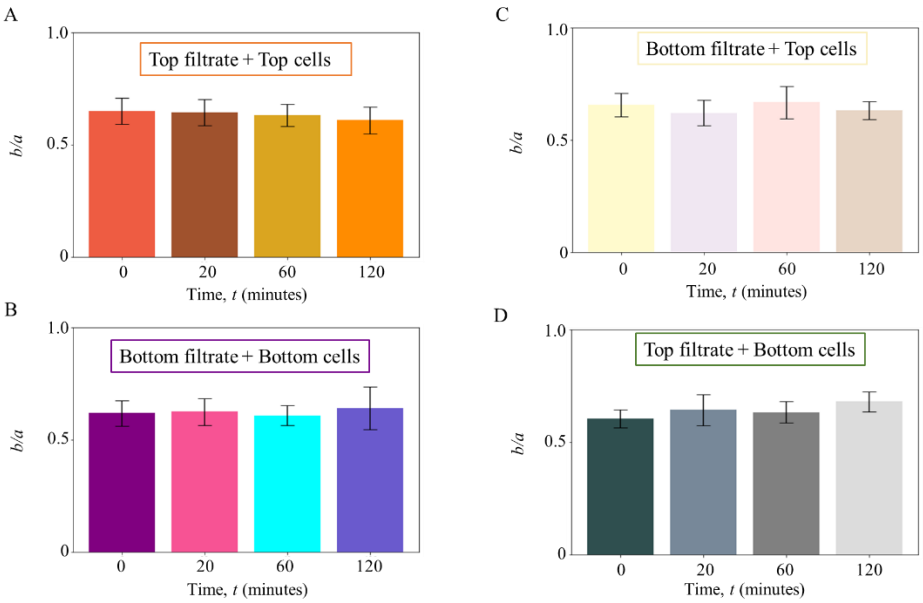

Fig. S15. *b/a* values of cells over time in presence of filtrates. (A) For top cells in presence of top filtrate *[T, T]*, the mean (± s.d.) values of *b/a* over 0, 20, 60 and 120 minutes are 0.65 ± 0.06, 0.64 ± 0.06, 0.63 ± 0.05 and 0.61 ± 0.06. **(B)** For bottom cells in presence of bottom filtrate *[B, B]*, the mean (± s.d.) values are 0.62 ± 0.06, 0.62 ± 0.06, 0.61 ± 0.05 and 0.64 ± 0.1. **(C)** For top cells in presence of bottom filtrate *[B, T]*, the mean (± s.d.) values are 0.66 ± 0.05, 0.62 ± 0.06, 0.67 ± 0.07 and 0.63 ± 0.04. **(D)** For bottom cells in presence of top filtrate *[T, B]*, the mean (± s.d.) values are 0.6 ± 0.04, 0.64 ± 0.07, 0.63 ± 0.05 and 0.68 ± 0.04.

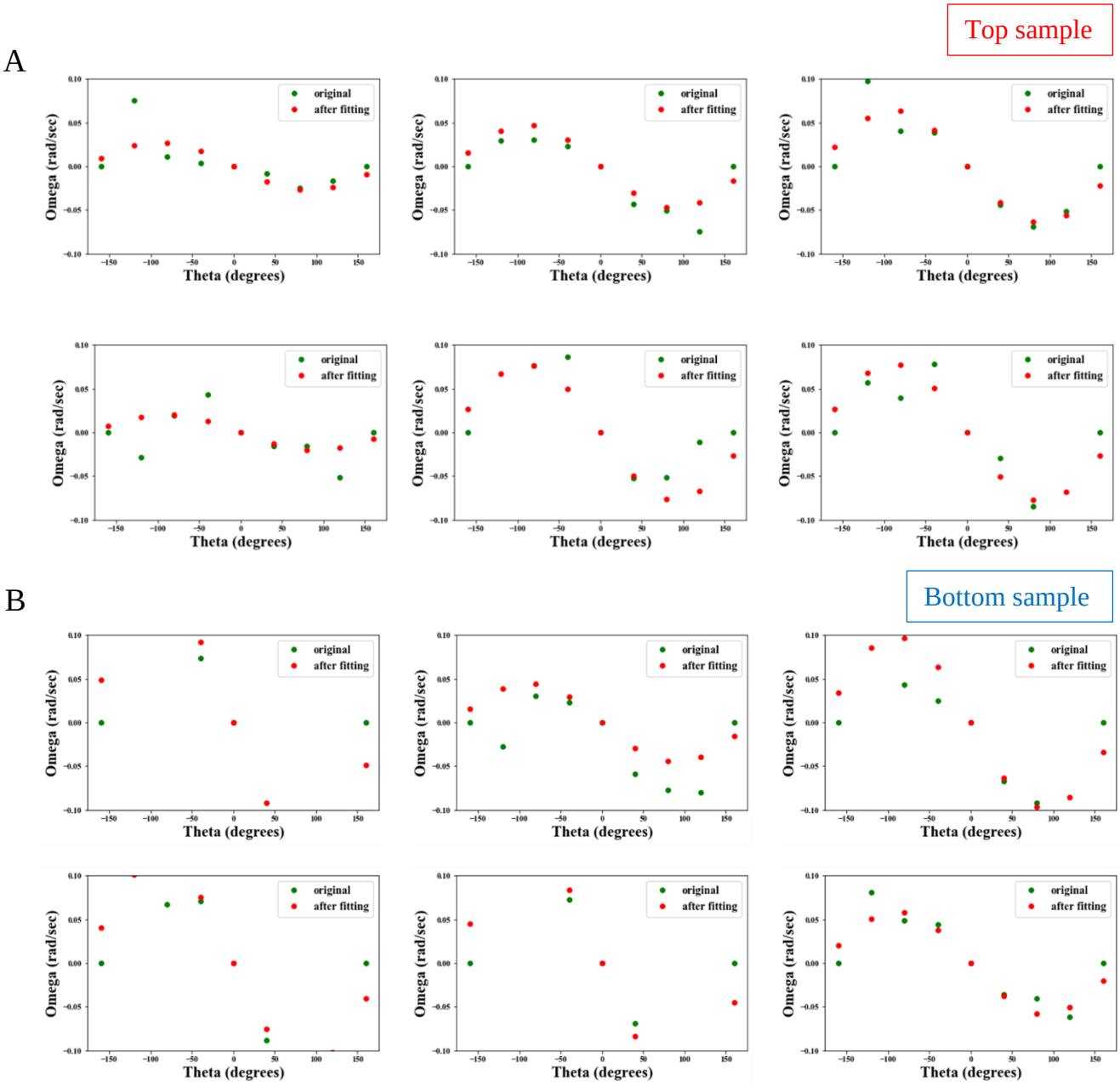

Fig. S16. Quantification of the orientational stability of cell samples during night. To compute the stability of top and bottom samples, rotation rate (ω) of cells were plotted as a function of the instantaneous angular direction (θ). The time of experiment was 00:00 h. **(A)** shows the stability of top cells with each panel corresponding to one replicate (of 6 replicates, as mentioned in Fig. S3). Red dots correspond to experimental data and green dots to the sinusoidal curve obtained by fitting a sinusoid to the experimental data. **(B)** shows the same but for bottom cells. The amplitude, A of the fitted curve was used to obtain the reorientation timescale, B as $B = \frac{1}{2A}$.

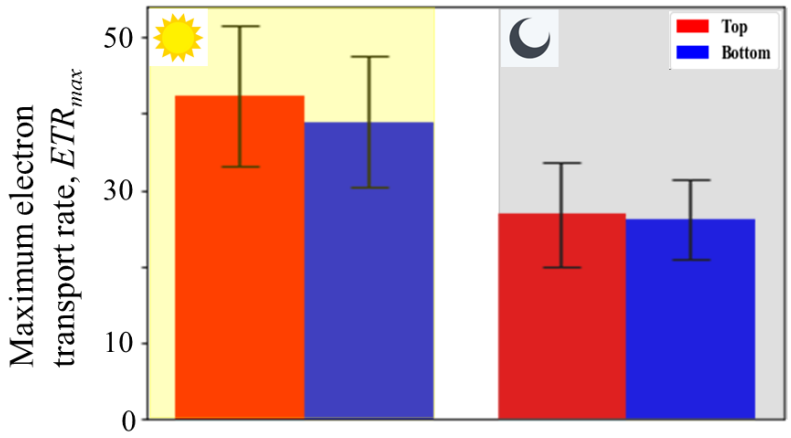

Fig. S17. Estimation of the electron transport rate (ETR_{max}) using the PAM device. Complementing the maximum photosynthetic yield and non-photochemical quenching, two key processes during light harvesting, this figure shows the maximum ETR, ETR_{max}, during the same. During daytime, the difference between top and bottom for this value is not statistically significant (p = 0.69). At night as well, there is no significant difference (p = 0.94).

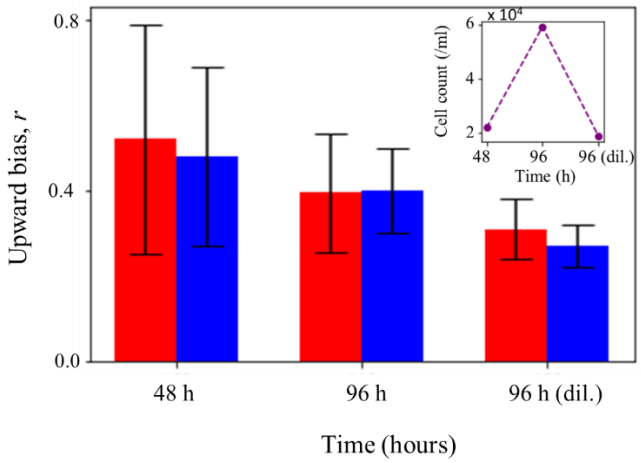

Fig. S18. Effect of cell concentration on swimming behavior. To study the effect of concentration on population behavior, two points in growth phase: 48 h and 96 h were chosen for which the upward bias (*r*) values were measured (cell counts are shown in the inset). At 48 h, both top (red bar) and bottom (blue bar) have higher mean (± s.d.) *r* than at 96 h. Same cells from 96-hour culture were taken and diluted (dil.) ~3 times with corresponding filtrate, to achieve a concentration comparable to that at 48 h (third data point, inset). The *r* value of this diluted sample was calculated and compared to the other two datasets. 4 replicates were used for 48 h and 96 h (diluted), and 6 at the 96 h timepoint.

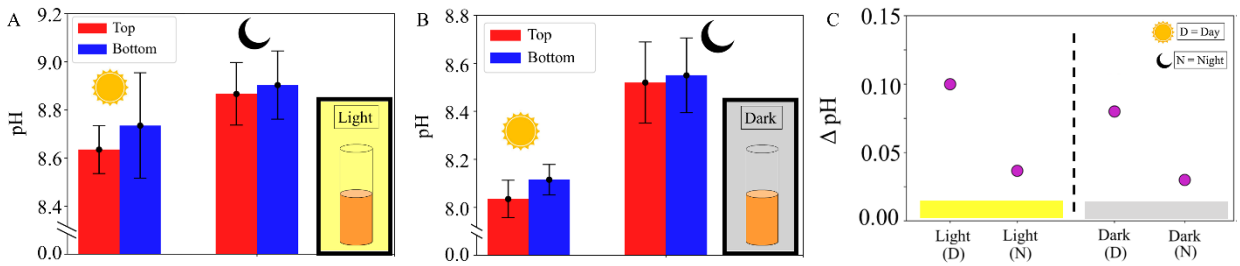

Fig. S19. pH changes result from endogenous rhythms independent of the environment. (A) Relative difference in pH between the top (red) and bottom (blue) sub-population regions of the column, measured during the day (D) and night (N) time for cell cultures kept under perpetual light conditions. (B) A similar trend was observed for the cell cultures kept under complete darkness. (C) Overall pH difference, ΔpH, across day and night time measurements for samples kept under complete light and dark settings. Sub-populations introduced to fresh media with precisely controlled and experimentally-relevant pH values (that are otherwise chemically identical), showed similar phenotypic trends (morphology and motility) as were observed for corresponding cells in the spent media. These results unambiguously demonstrate that the local pH causes the alteration of the swimming behavior.